

**Nuclear Imaging with $^{188}\text{Re}(\text{V})$ -*meso*-DMSA and
 $^{188}\text{Re}(\text{V})$ -*rac*-DMSA in nude mice xenografted with
a neuroendocrine tumor cells**

Jun Young Park

**The Graduate School
Yonsei University
Department of Biomedical Laboratory Science**

**Nuclear Imaging with $^{188}\text{Re(V)}$ -*meso*-DMSA and
 $^{188}\text{Re(V)}$ -*rac*-DMSA in nude mice xenografted with
a neuroendocrine tumor cells**

A Masters Thesis

Submitted to the Department of Biomedical
Laboratory Science and the Graduate School of
Yonsei University

in partial fulfillment of the
requirements for the degree of
Master of Science

Jun Young Park

December 2006

**This certifies that the masters thesis of
Jun Young Park is approved.**

Thesis Supervisor : Ok Doo Awh

Tae Woo Kim : Thesis Committee Member

Yong Serk Park : Thesis Committee Member

The Graduate School
Yonsei University
December 2006

- Intelligence without ambition is a bird without wings -

Salvador Dali

- Life is what happens to you, While you're busy making other plans -

John Lennon

for Mom, Daddy

&

Special thanks to Prof. Awh O.D., Phd. Choi T.H., Phd. Lee T.S.

CONTENTS

LIST OF FIGURES	iii
LIST OF TABLES	iv
ABBREVIATION	v
ABSTRACT IN ENGLISH	vi
I. INTRODUCTION	1
II. MATERIALS AND METHODS	6
1. Materials	6
2. Methods	7
2.1. Synthesis of <i>rac</i> -2,3-Dimercaptosuccinic Acid	7
2.1.1. <i>rac</i> -Bis(thioacetyl) succinic Acids	7
2.1.2. <i>rac</i> -2,3-Dimercaptosuccinic Acids	7
2.2. Preparation of ¹⁸⁸ Re(V)-DMSA complexes	8
2.2.1. ¹⁸⁸ Re(V)- <i>meso</i> -DMSA complexes	8
2.2.2. ¹⁸⁸ Re(V)- <i>rac</i> -DMSA complexes	9
2.3. Chromatographic analysis of ¹⁸⁸ Re(V)-DMSA complexes	9
2.4. Biochemical Characterizations of ¹⁸⁸ Re(V)-DMSA complexes	11
2.4.1. <i>in vitro</i> Stability	11
2.4.2. Lipophilicity	11
2.4.3. Bindability to Protein	12
2.5. Organ Distribution of ¹⁸⁸ Re(V)-DMSA complexes in nude mouse bearing PC-12	12
2.5.1. Cell culture and tumor implantation	12
2.5.2. Organ distribution studies	13

2.6. Gamma camera Image with $^{188}\text{Re(V)}$ -DMSA complexes in nude mouse bearing PC-12	14
III. RESULTS	15
1. Synthesis of <i>rac</i> -2,3-Dimercaptosuccinic Acid	15
2. Preparation of $^{188}\text{Re(V)}$ -DMSA complexes	15
2.1. $^{188}\text{Re(V)}$ - <i>meso</i> -DMSA complexes	15
2.2. $^{188}\text{Re(V)}$ - <i>rac</i> -DMSA complexes	16
3. Chromatographic analysis of $^{188}\text{Re(V)}$ -DMSA complexes	23
4. Biochemical Characterizations of $^{188}\text{Re(V)}$ -DMSA complexes	29
5. Organ Distribution of $^{188}\text{Re(V)}$ -DMSA complexes in nude mouse bearing PC-12	32
6. Gamma camera Image with $^{188}\text{Re(V)}$ -DMSA complexes in nude mouse bearing PC-12	37
IV. DISCUSSION	41
V. CONCLUSION	45
VI. REFERENCE	47
ABSTRACT IN KOREAN	52

LIST OF FIGURES

Fig. 1. Production and decay mechanisms of ^{188}Re in generator system	1
Fig. 2. The chemical structure of DMSA	2
Fig. 3. Synthetic scheme of diastereomeric DMSA	3
Fig. 4. Synthetic scheme of diastereomeric $^{188}\text{Re(V)}$ -DMSA complexes	10
Fig. 5. Effect of MBS concentration on the yield of $^{188}\text{Re(V)}$ - <i>meso</i> -DMSA	17
Fig. 6. Effect of 2,3- <i>meso</i> -DMSA concentration on the yield of $^{188}\text{Re(V)}$ - <i>meso</i> -DMSA	18
Fig. 7. Effect of pH on the yield of $^{188}\text{Re(V)}$ - <i>meso</i> -DMSA	19
Fig. 8. Effect of MBS concentration on the yield of $^{188}\text{Re(V)}$ - <i>rac</i> -DMSA	20
Fig. 9. Effect of 2,3- <i>rac</i> -DMSA concentration on the yield of $^{188}\text{Re(V)}$ - <i>rac</i> -DMSA	21
Fig. 10. Effect of pH on the yield of $^{188}\text{Re(V)}$ - <i>rac</i> -DMSA	22
Fig. 11. Radiochromatogram of $^{188}\text{Re(V)}$ - <i>meso</i> -DMSA	24
Fig. 12. Radiochromatogram of $^{188}\text{Re(V)}$ - <i>rac</i> -DMSA	25
Fig. 13. HPLC chromatogram of $^{188}\text{Re(V)}$ - <i>meso</i> -DMSA	27
Fig. 14. HPLC chromatogram of $^{188}\text{Re(V)}$ - <i>rac</i> -DMSA	28
Fig. 15. <i>in vitro</i> Stability test of $^{188}\text{Re(V)}$ -DMSA complexes	30
Fig. 16. Biodistribution of $^{188}\text{Re(V)}$ - <i>meso</i> -DMSA in nude mouse bearing PC-12	34
Fig. 17. Biodistribution of $^{188}\text{Re(V)}$ - <i>rac</i> -DMSA in nude mouse bearing PC-12	36
Fig. 18. Gamma camera image of $^{188}\text{Re(V)}$ - <i>meso</i> -DMSA in nude mouse bearing PC-12	39
Fig. 19. Gamma camera image of $^{188}\text{Re(V)}$ - <i>rac</i> -DMSA in nude mouse bearing PC-12	40

LIST OF TABLES

Table 1. The optimal conditions for the preparation of $^{188}\text{Re(V)}$ -DMSA complexes ...	26
Table 2. Lipophilicity and protein bindability of $^{188}\text{Re(V)}$ -DMSA complexes	31
Table 3. Biodistribution of $^{188}\text{Re-meso}$ -DMSA in nude mouse bearing PC-12 ...	33
Table 4. Biodistribution of $^{188}\text{Re-rac}$ -DMSA in nude mouse bearing PC-12	35
Table 5. Organ per Tissue ratios of $^{188}\text{Re(V)}$ -DMSA complexes	38

ABBREVIATION

Re : rhenium

Tc : technetium

DMSA : dimercaptosuccinic acids

rac : racemic

MBS : sodium metabisulfite

TLC-SG : thin layer chromatography - silica gel

NMR : nuclear magnetic resonance

HPLC : high performance liquid chromatography

% ID/g : % injected dose/gram tissue

CFU : colony forming units

ABSTRACT

Nuclear Imaging with $^{188}\text{Re(V)}$ -*meso*-DMSA and $^{188}\text{Re(V)}$ -*rac*-DMSA in nude mice xenografted with a neuroendocrine tumor cells

Rhenium-188 is a very attractive radioisotope for a variety of therapeutic and diagnostic applications in nuclear medicine. Dimercaptosuccinic acid (DMSA) exists in the *meso* or *racemic* (*rac*) form. In this study, ^{188}Re complexes with diastereomeric DMSA were prepared to compare the property of $^{188}\text{Re(V)}$ -*rac*-DMSA with $^{188}\text{Re(V)}$ -*meso*-DMSA in *in vitro* and *in vivo* models and to evaluate their possible use as a tumor diagnostic and therapeutic agent.

rac-2,3-DMSA was synthesized through two steps with 14% yields. $^{188}\text{Re(V)}$ -DMSA complexes were prepared from *meso*- and *rac*-2,3-DMSA by labeling with ^{188}Re in the presence of sodium metabisulfite (MBS, $\text{Na}_2\text{S}_2\text{O}_5$). For maximum yields, $^{188}\text{Re(V)}$ -*rac*-DMSA was needed a higher concentration of MBS and *rac*-2,3-DMSA. $^{188}\text{Re(V)}$ -*meso*-DMSA showed high labeling efficiency at pH 2, whereas $^{188}\text{Re(V)}$ -*rac*-DMSA was prepared at pH 5 for maximum yields. Both $^{188}\text{Re(V)}$ -*meso*-DMSA and $^{188}\text{Re(V)}$ -*rac*-DMSA showed excellent radiochemical purity and stability at room temperature.

$^{188}\text{Re(V)-meso-DMSA}$ observed more lipophilic than $^{188}\text{Re(V)-meso-DMSA}$. In serum protein binding assay, $^{188}\text{Re(V)-meso-DMSA}$ and $^{188}\text{Re(V)-rac-DMSA}$ showed almost similar property. Tumor uptakes of $^{188}\text{Re(V)-rac-DMSA}$ and $^{188}\text{Re(V)-meso-DMSA}$ in xenografted nude mice were 1.15 %ID/g and 0.40 %ID/g at 1h post injection, respectively. The gamma camera image of $^{188}\text{Re(V)-rac-DMSA}$ showed more selectively localized than $^{188}\text{Re(V)-meso-DMSA}$ on tumor region in xenografted nude mice.

These results demonstrated that $^{188}\text{Re(V)-rac-DMSA}$ may have better potential than $^{188}\text{Re(V)-meso-DMSA}$ as a diagnostic and therapeutic agent for treatment of neuroendocrine tumor.

Keywords : ^{188}Re , DMSA, neuroendocrine tumor, radiopharmaceuticals, radiotherapy

I. INTRODUCTION

Rhenium-188 is a very attractive radioisotope for a variety of therapeutic applications in nuclear medicine, oncology and interventional cardiology, particularly because of its favorable nuclear properties.[1,2] Rhenium-188 (^{188}Re , $t_{1/2} = 16.9\text{h}$) decays by the emission of a β -particle ($E_{\beta} = 2.11\text{ MeV}$), which has a high energy appropriate for penetrating and destroying abnormal tissues, and γ -rays ($E_{\gamma} = 155\text{ keV}$), which can be useful for dosimetry and monitoring of tumor uptake using gamma camera imaging. In addition, ^{188}Re is conveniently obtained from in-house $^{188}\text{W}/^{188}\text{Re}$ generator system.[3] The $^{188}\text{W}/^{188}\text{Re}$ generator is based on ^{188}Re separation from ^{188}W using an alumina column. The parent nuclide, ^{188}W , is loaded on the column and it decays to ^{188}Re with a half-life of 69 days. Consequently, the carrier-free ^{188}Re daughter radionuclide is obtained as sodium perrhenate ($\text{Na}[^{188}\text{ReO}_4]$) by elution of the generator with normal saline (Fig. 1).

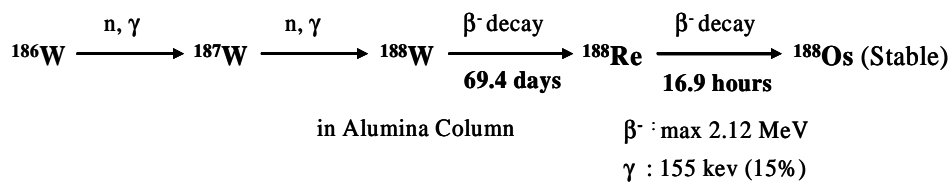


Figure 1. Production and decay mechanisms of ^{188}Re in generator system.

Technetium-99m (^{99m}Tc , $t_{1/2} = 6\text{h}$, $E_{\gamma} = 140\text{ keV}$) is most widely used radioisotope in nuclear diagnostic imaging. Since technetium and rhenium is comprised in Group VIIA of periodic table, the physicochemical properties of rhenium is similar to that of technetium. For this reason, ^{188}Re can be readily prepared by the labeling methods that have been developed for ^{99m}Tc radiopharmaceuticals.

DMSA is the compound contained two mercapto and two carboxylic groups which has a ability to interact with metals and form internal complexes (Fig. 2). The earlier studies identified DMSA forms complexes with zinc, nickel, cobalt, cadmium and copper, however, it does not form complexes with ions of the alkaline earth metals.[4]

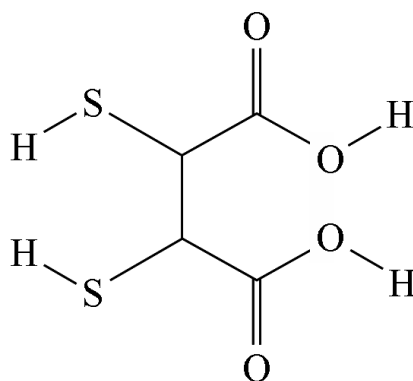


Figure 2. The chemical structure of DMSA.

DMSA exists in two diastereoisomeric forms, *meso* and *rac*. DMSA diastereomers were synthesized from acetylene dicarboxylic acid and thioacetic

acid (Fig. 3). [5,6]

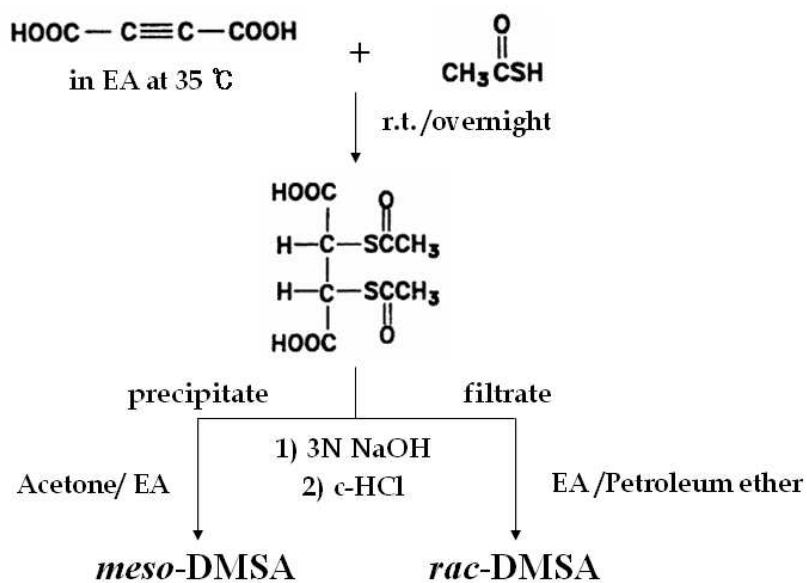


Figure 3. Synthetic scheme of diastereomeric DMSA.

The *meso*-2,3-DMSA and its metal chelates have been extensively studied in China, Russia and United state since the 1950s.[7-9] The *meso*-2,3-DMSA is approved by the Food and Drug Administration for treatment of lead and mercury intoxication both in children and adults. Compared to the *meso* form, however, *rac*-2,3-DMSA has received little attention because of the difficulty in the synthesis of the *racemic* form. Unlike *meso* isomer, *rac*-2,3-DMSA is very soluble in water, strongly acidic solutions and in organic solvents. The

crystal structure of *rac*-2,3-DMSA exists as a double-stranded structure in which each molecule is in a gauche configuration. However, *meso*-2,3-DMSA exists in a single strand in which each molecule has adopted an anti configuration and the individual molecules are joined together at each end by hydrogen bond. These differences in the conformations may be responsible for the higher solubility of *rac*-2,3-DMSA in aqueous solutions.[10]

Neuroendocrine tumors (NETs) are a heterogeneous group of neoplasms that originate from endocrine glands, endocrine islets and cells dispersed between exocrine cells.[11,12] These tumors are rare, slow-growing and retain many multipotent differentiation capacities.[13] NETs are characterized by the presence of neuroamine uptake mechanisms as well as peptide receptors and transporters at the cell membrane and these features constitute the basis of the clinical use of specific radiolabeled ligands, both for imaging and therapy.[14] Common types of NETs are carcinoids, other pancreatic islet cell tumors, melanomas, pheochromocytoma and medullary thyroid carcinomas (MTC).[15] $^{99m}\text{Tc(V)}$ -DMSA has been already adapted as an imaging agent for MTC.[16-19] And preliminary study of $^{186}\text{Re(V)}$ -*meso*-DMSA in MTC showed that its general biodistribution characteristics and avidity are similar to those of $^{99m}\text{Tc(V)}$ -DMSA.[20] This analogy suggests that $^{188}\text{Re(V)}$ -DMSA complexes may also have potential of application in imaging and targeted radiotherapy of NETs.

In this study, the *rac*-2,3-DMSA was synthesized to investigate the optimal reaction conditions for high labeling yields of $^{188}\text{Re(V)}$ -*rac*-DMSA. In addition, we compared the *in vivo* behaviors of $^{188}\text{Re(V)}$ -*rac*-DMSA with $^{188}\text{Re(V)}$ -*meso*-DMSA in athymic nude mice bearing the PC-12 neuroendocrine tumor for evaluating

the possibility of $^{188}\text{Re(V)}$ -DMSA complexes as a therapeutic and diagnostic agent.

II. MATERIALS AND METHODS

1. Materials

Acetylene dicarboxylic acid, thioacetic acid, ethylacetate, diethylether, sodium metabisulfite, *meso*-2,3-dimercaptosuccinic acid, chloroform, Na₂CO₃, MgSO₄ were purchased from Sigma-Aldrich Co. (St. Louis, USA). Acetone, HCl, Thin layer chromatography (TLC ; Silica gel 60, F₂₅₄) were purchased from Merck (Darmstadt, Germany). Benzene and petroleum ether were purchased from Junsei chemicals (Tokyo, Japan). ¹⁸⁸Re-perrhenate (¹⁸⁸ReO₄⁻) was eluted from a ¹⁸⁸W/¹⁸⁸Re generator provided by Oak Ridge National Laboratory (Oak Ridge, USA). IC-Ag cation exchange cartridges were purchased from Alltech Associates (Deerfield, USA) and QMA SepPak cartridge ion exchange columns were obtained from Waters Corporation (Milford, USA)

Melting points were taken on a Electrothermal MEL-TEMP apparatus (Barnstead Thermolyne, USA). ¹H-NMR spectra were recorded on a AC-100F 100MHz NMR spectrometer (Bruker, Germany). HPLC analysis was performed using a Waters gradient LC system consisting of a dual head 515 pump, 484 UV detector (Waters, USA) and GABI RI-detector (Raytest, Germany). The 150×4.1mm PRP-1 column (Hamilton, USA) was used for HPLC analysis. The radiochemical purity was tested by a Thin-layer chromatogram scanner (Aloka, Japan). The radioactivity was counted on a 1480 WIZARD well-type gamma counter (Wallac, Finland) and image was obtained with a gamma camera (TRIAD TXLT-20, Trionix, USA).

Ham's F12K medium was purchased from Gibco BRL (Grand Island, USA). Female athymic Balb/C *nu/nu* mice were obtained from Central Laboratory Animal Inc (Seoul, Korea).

2. Methods

2.1. Synthesis of *rac*-2,3-Dimercaptosuccinic Acid

2.1.1. *rac*-Bis(thioacetyl) succinic Acids

Acetylene dicarboxylic acid (10 g, 87.7 mmol) was dissolved in 31.6 ml of ethylacetate at 35°C. Thioacetic acid (8.6 g, 175.4 mmol) was added slowly into this solution. A white precipitate formed in approximately 3 h. The solution was stirred overnight at room temperature. The reaction mixture was filtered and the filtrate was concentrated under the reduced pressure. The residual oily product was crystallized from ethylacetate/petroleum ether several times to obtain 2.1 g of *rac*-Bis(thioacetyl) succinic Acids. The purity of the compound was checked by melting point and ¹H-NMR.

2.1.2. *rac*-2,3-Dimercaptosuccinic Acids

rac-Bis(thioacetyl) succinic acid (4.2 g, 12.8 mmol) was dissolved to 3 N NaOH (28 ml) and stirred vigorously for 3 min. The mixture was cooled to 0°C and acidified with 10 N HCl. After standing for 1 h, the reaction mixture was filtered and extracted with diethylether several times. The organic phase

was dried over Na_2SO_4 and concentrated under the reduced pressure. The resulting oily product was crystallized from diethylether/benzene. The greenish yellow solid was purified by repeated recrystallization from the above solvent to give 1.5 g of *rac*-2,3-dimercaptosuccinic acid. The purity of the compound was checked by melting point and $^1\text{H-NMR}$.

2.2. Preparation of $^{188}\text{Re(V)}$ -DMSA complexes

2.2.1. $^{188}\text{Re(V)}$ -*meso*-DMSA complex

^{188}Re was obtained from an alumina-based $^{188}\text{W}/^{188}\text{Re}$ generator. Elution of the $^{188}\text{W}/^{188}\text{Re}$ generator with 10 ml of normal saline provided solutions of carrier-free ^{188}Re as sodium perrhenate (NaReO_4). "Carrier free" means radionuclide was not diluted with a stable isotope of similar form. For the preparation of highly concentrated ^{188}Re solutions, the generator eluents were first passed through a IC-Ag cation-exchange cartridge that selectively removes chlorides ions by forming insoluble silver chloride, and then resulting eluents were passed through a SepPak anion-trapping column. The ^{188}Re -perrhenate were obtained by elution of the SepPak column with 1.0 ml normal saline.

10 mg of *meso*-2,3-DMSA was dissolved in 0.1 ml of argon purged distilled water, and then 0.2 ml (100 μg , 0.54 μM , 4 mCi) of $^{188}\text{ReO}_4^-$ solution was mixed in a 10 ml vial. To this mixture, 30 mg of sodium metabisulfite (0.15 mM) dissolved in a 0.30 ml of normal saline was added. The pH of the complex was adjusted to 3.5 by addition of 1 N NaOH. The reaction mixture

appeared turbid, because *meso*-2,3-DMSA is more soluble in the basic condition than acidic. Turbidity disappeared after purging with argon for 3 min. The vial was sealed and incubated at 80°C for 60 min and allowed to cool to room temperature. Various experiments were carried out to optimize the labelling conditions for getting a maximum complexation yield. These include the effect of DMSA concentration, sodium metabisulfite concentration, pH of the reaction mixture, incubation time.

2.2.2. $^{188}\text{Re(V)}$ -*rac*-DMSA complex

Exactly the same procedures and labelling conditions for the preparation of $^{188}\text{Re(V)}$ -*meso*-DMSA were followed starting with *rac*-2,3-DMSA instead of *meso*-2,3-DMSA. Since *rac*-2,3-DMSA is very soluble in water, there was no need for argon purging procedure. The preparation of $^{188}\text{Re(V)}$ -DMSA complexes is summarized in Figure 4.

2.3. Chromatographic analysis of $^{188}\text{Re(V)}$ -DMSA complexes

TLC was examined to investigate the radiolabeling yield and radiochemical purity of $^{188}\text{Re(V)}$ -DMSA complexes. TLC media was silica gel type. The plates were cut into 2 × 10 cm strips. 3 μl portion of the test solutions were applied at 1.5 cm from the lower end of the TLC plate. The strip was developed with 0.9% saline solution and acetone. To determine the labelling yield of $^{188}\text{Re(V)}$ -DMSA complexes, plates were scanned and analyzed with a TLC scanner.

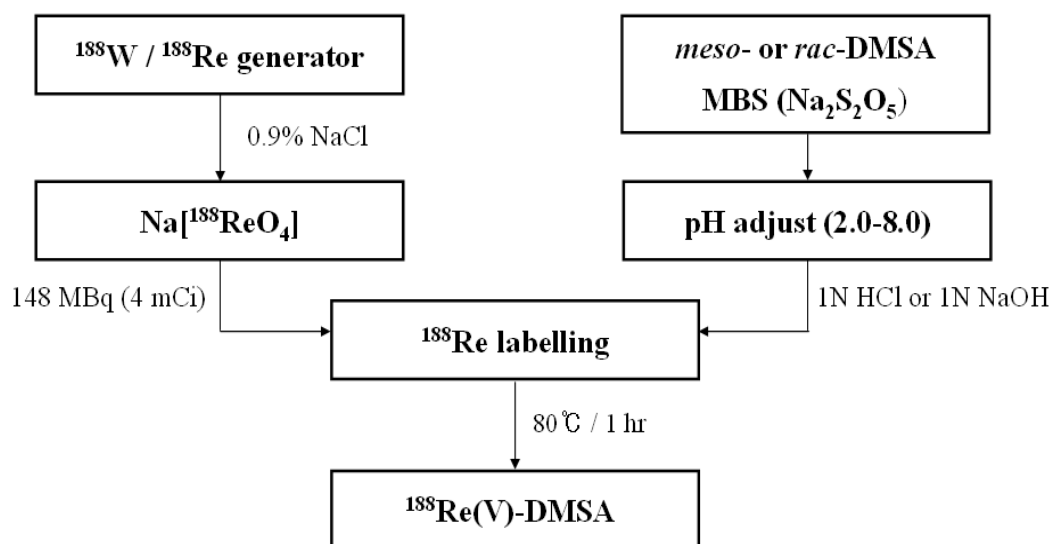


Figure 4. Synthetic scheme of diastereomeric $^{188}\text{Re(V)-DMSA}$ complexes.

The preparations were also analysed by reversed phase high performance liquid chromatography. The reversed phase HPLC was performed on a Hamilton PRP-1 column with a gradient elution system comprising 0.1% trifluoroacetic acid in water (solvent A) and 0.1% trifluoroacetic acid in acetonitrile (solvent B). The flow rate was 1 ml/min and the gradient was as follows : 0 min, 0% B; 1 min, 0% B; 12 min, 25% B; 14 min, 25% B; 16 min, 0% B. The peaks were monitored by a UV detector at 340 nm and by a gamma radioactivity detector.

2.4. Biochemical Characterizations of $^{188}\text{Re(V)}$ -DMSA complexes

2.4.1. *in vitro* Stability

The stability of the $^{188}\text{Re(V)}$ -DMSA complexes prepared under the optimized conditions was determined at various time points (0, 1, 2, 3, 6, 18, 24 h). The pH values of the samples were adjusted to 7.5 with 1 N NaOH. The complexes were incubated for 24 h at room temperature and analyzed by TLC using 0.9% saline solution and acetone as developer.

2.4.2. Lipophilicity

The lipophilic properties of the $^{188}\text{Re(V)}$ -DMSA complexes were characterized by the distribution between water and n-octanol as a organic phase. Partition coefficient was measured by the following manner. 1 ml of 0.9% saline solution was added to 1 ml of n-octanol. 0.01 ml of

$^{188}\text{Re(V)}$ -DMSA solution was added to the above solution and mixed for 10 min. The mixture was allowed to stand at room temperature for 1 h. After incubation, aliquots (10 μl) of each phase were removed and assayed from their radioactivities in a well type gamma counter. The radioactivity ratio in cpm/ml of n-octanol to that of aqueous layer was calculated and the distribution coefficients were determined. Distribution was obtained by logarithm of distribution coefficient.

2.4.3. Bindability to Protein

Serum protein binding activities of the $^{188}\text{Re(V)}$ -DMSA complexes were examined in the following manner. 500 μl of human serum were mixed with 10 μl of $^{188}\text{Re(V)}$ -DMSA (total radioactivity, T) and the mixture was incubated at 37°C for 1 h. 500 μl of 20% trichloroacetic acid in water (w/v) were added to the mixture in order to precipitate serum proteins. The mixture was vortexed and centrifuged at $2,500 \times g$ for 10 min, and the supernatant was removed. The radioactivity of the precipitate (bound radioactivity, B) was counted in a well type gamma counter and the protein bindability (B/T, %) was calculated.

2.5. Organ distribution of $^{188}\text{Re(V)}$ -DMSA complexes in nude mouse bearing PC-12

2.5.1. Cell culture and tumor implantation

The rat pheochromocytoma cell line PC-12 was obtained from the

American Type Culture Collection (ATCC, Manassas, USA). PC-12 cells were grown in Ham's F12K medium containing 15% inactivated horse serum, 2.5% fetal bovine serum (Gibco BRL) and 1% streptomycin. Cells were maintained as monolayers in 175 cm² tissue culture flasks at 37°C under a humidified atmosphere of 5% CO₂ / 95% O₂. The medium was changed every 2-3 days.

Five- to six-week-old female athymic BALB/c *nu/nu* mice were used for tumor implantation studies. For implantation, PC-12 cells in log phase of growth were harvested with trypsin 0.25% and EDTA 0.02%. After checking cell viability with the trypan blue-dye exclusion test, the cells were counted with a hemacytometer and adjusted to 3×10^8 cells/ml in the 0.9% saline. They were kept cold until use. Each animal was inoculated subcutaneously with 100 μ l tumor suspension on the right flank. Tumor growth was monitored at least twice a week and tumor size was calculated by multiplying the length and width of the tumor on a given day. Organ distribution was conducted when each tumor reached a diameter of 5×10 mm at 4-5 weeks after tumor implantation.

2.5.2. Organ distribution studies

All animal studies were performed with the approval of the Korea Institute of Radiological and Medical Sciences (KIRAMS) Animal Care and Use Committee. Organ distribution of the ¹⁸⁸Re(V)-DMSA complexes was evaluated in xenotransplanted nude mice. The pH of the ¹⁸⁸Re(V)-DMSA complexes was adjusted to 7.5 prior to injection. Each tumored mouse was injected via a lateral tail vein with 0.1 ml of complex solution containing

approximately 10 mCi (0.37 MBq) of activity. The mice were sacrificed by diethylether overdose at times of 1, 3 and 24 h after injection. Blood was collected by cardiac puncture and the samples of liver, lung, spleen, kidney, stomach, intestine, muscle, and tumor were taken carefully. The thyroid was generally isolated with surrounding tissues of the neck and the left femur was isolated as a representative bone sample. Organ samples were immediately weighed and counted in a well-type gamma counter to calculate resident activity in different organs. The accumulated activity was expressed as percent injected dose per gram of tissue (% *Injected dose/g*).

2.6. Gamma camera Image of $^{188}\text{Re(V)}$ -DMSA complexes in nude mouse bearing PC-12

Nuclear image of $^{188}\text{Re(V)}$ -DMSA complexes was obtained with gamma camera in nude mice bearing PC-12 neuroendocrine tumors. Approximately 400 mCi (14.8 MBq) of activity was administrated through a tail vein. At 1, 3 and 6 h after injection, the animals were anesthetized by intraperitoneal injection of a mixture of ketamine (1.6 mg/mouse) and xylazine (240 μg /mouse) in saline. Tumor images were acquired each for 1×10^6 counts in a 256×256 matrix.

III. RESULTS

1. Synthesis of *rac*-2,3-Dimercaptosuccinic Acid

rac-2,3-DMSA was synthesized from two step procedures almost similar to Gerecke's synthesis.[21] *rac*-2,3-DMSA was obtained from *rac*-Bis(thioacetyl) succinic Acids. The yield of *rac*-Bis(thioacetyl) succinic Acids was 10% and its melting point was 145-149°C. In the ¹H-NMR spectroscopy, the two resonance peaks at 2.40 and 4.67 ppm were present and the ratio of these two peaks was about 3:1. The *rac*-2,3-DMSA was purified by recrystallization from diethylether and benzene. The yield of *rac*-2,3-DMSA was 14%. Melting point was 123-127°C and ¹H-NMR showed two main peaks at 2.4 and 3.7 ppm.

2. Preparation of ¹⁸⁸Re-DMSA complexes

2.1. ¹⁸⁸Re(V)-*meso*-DMSA complexes

Various experiments were carried out to optimize the radiolabeling conditions for getting a maximum complexation yield. The labelling efficiency of ¹⁸⁸Re(V)-*meso*-DMSA was checked by TLC chromatographic system. The effect of MBS concentration was carried out at pH 3.5 with 10 mg of *meso*-2,3-DMSA. It was observed that ¹⁸⁸Re(V)-*meso*-DMSA was formed in high yield from 30 mg of MBS as a reducing agent (Fig. 5).

The effect of DMSA concentration was studied at pH 3.5 with 30 mg of

MBS. The yield of $^{188}\text{Re(V)-meso-DMSA}$ was 99.5% even at 10 mg of *meso*-2,3-DMSA (Fig. 6). The effect of pH was studied by adjusting with 1 N HCl or 1 N NaOH. The pH with maximum yield of $^{188}\text{Re(V)-meso-DMSA}$ was at 3.5 and the complexation yield of 99.5% could be achieved. However, radiolabeling yield of $^{188}\text{Re(V)-meso-DMSA}$ was rapidly decreased in alkaline pH values (Fig. 7). All studies on optimization of pH and reagent concentrations were carried out at 80°C for 1 h.

2.2. $^{188}\text{Re(V)-rac-DMSA}$ complexes

The same procedures and labelling conditions were examined in the preparation of $^{188}\text{Re(V)-rac-DMSA}$. The effect of MBS concentration was carried out at pH 3.5 with 10 mg of *rac*-2,3-DMSA. It was observed that the yield of $^{188}\text{Re(V)-rac-DMSA}$ was only 70% at 30 mg of MBS, however, over the 90% of yield was obtained from the use of 45 mg of MBS. And the optimum amount of MBS required for complexation was 90 mg (Fig. 8). The effect of *rac*-2,3-DMSA concentration was studied at pH 3.5 with 60 mg of MBS. The yield of $^{188}\text{Re(V)-rac-DMSA}$ was 94% at 10 mg of *rac*-2,3-DMSA. However, the yield was increased to 98% with 15 mg of *rac*-2,3-DMSA (Fig. 9). The pH with maximum yield of $^{188}\text{Re(V)-rac-DMSA}$ was at 5 and the complexation yield of 99.8% could be achieved (Fig. 10).

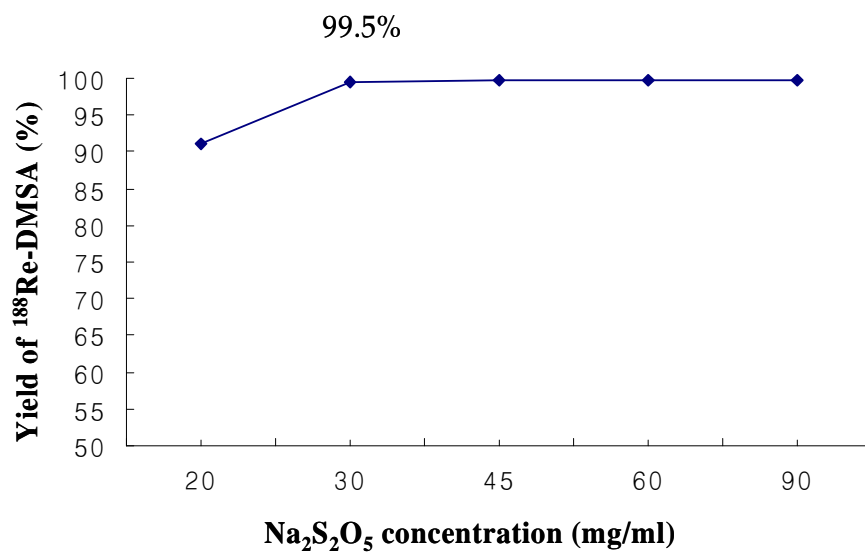


Figure 5. Effect of MBS concentration on the yield of $^{188}\text{Re(V)-meso-DMSA}$.

($^{188}\text{ReO}_4^-$: 4 mCi, DMSA : 10 mg/ml, pH 3.5, 80°C, 1h)

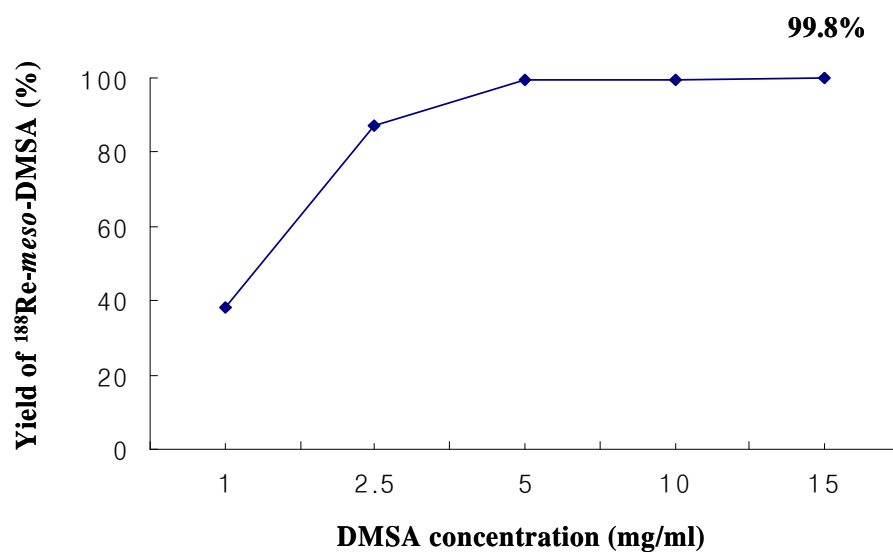


Figure 6. Effect of 2,3-*meso*-DMSA concentration on the yield of $^{188}\text{Re(V)-meso-DMSA}$.
($^{188}\text{ReO}_4^-$: 4 mCi, MBS : 30 mg/ml, pH 3.5, 80 °C, 1h)

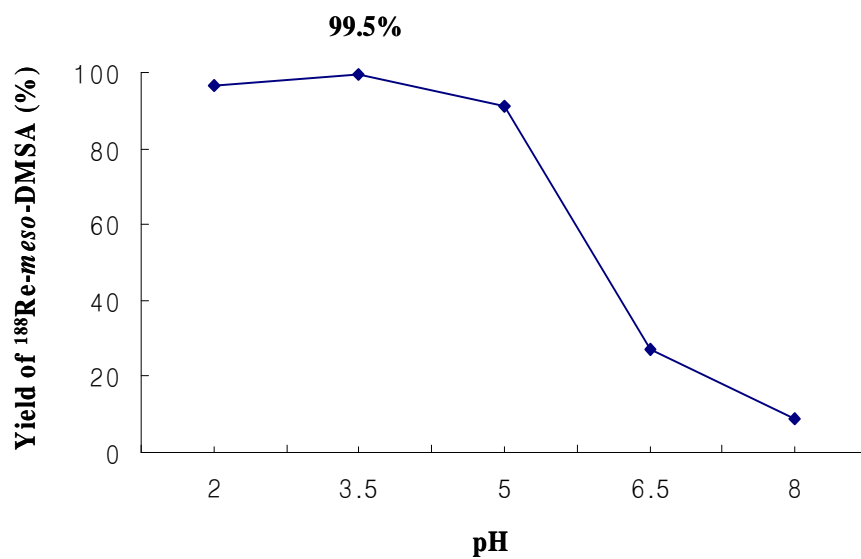


Figure 7. Effect of pH on the yield of $^{188}\text{Re(V)-meso-DMSA}$.

($^{188}\text{ReO}_4^-$: 4 mCi, DMSA : 10 mg/ml, MBS : 30 mg/ml, 80°C, 1h)

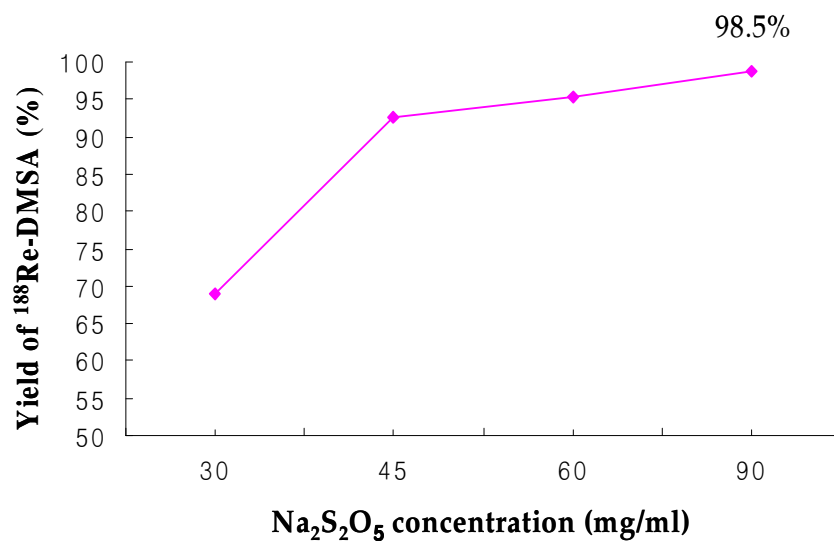


Figure 8. Effect of MBS concentration on the yield of $^{188}\text{Re(V)-rac-DMSA}$.

($^{188}\text{ReO}_4^-$: 4 mCi, DMSA : 10 mg/ml, pH 3.5, 80°C, 1h)

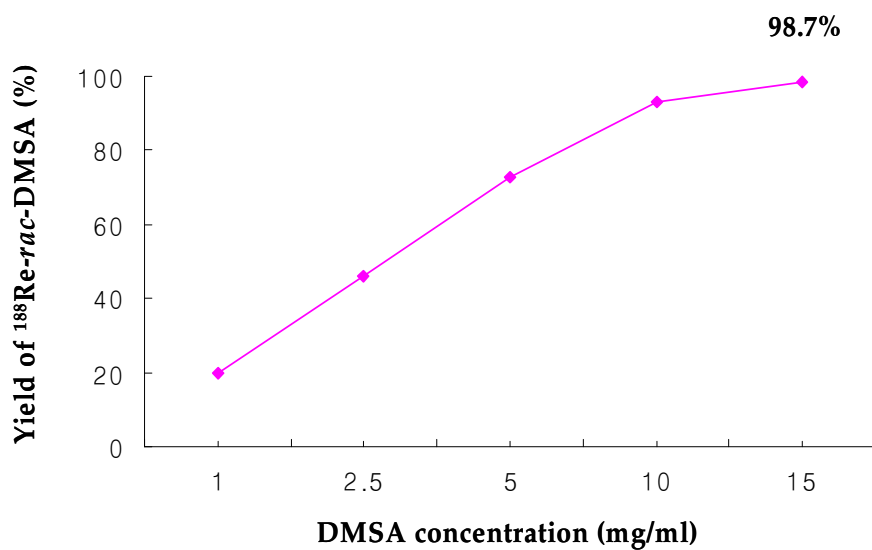


Figure 9. Effect of *rac*-2,3-DMSA concentration on the yield of $^{188}\text{Re(V)-rac-DMSA}$.

($^{188}\text{ReO}_4^-$: 4 mCi, MBS : 60 mg/ml, pH 3.5, 80°C, 1h)

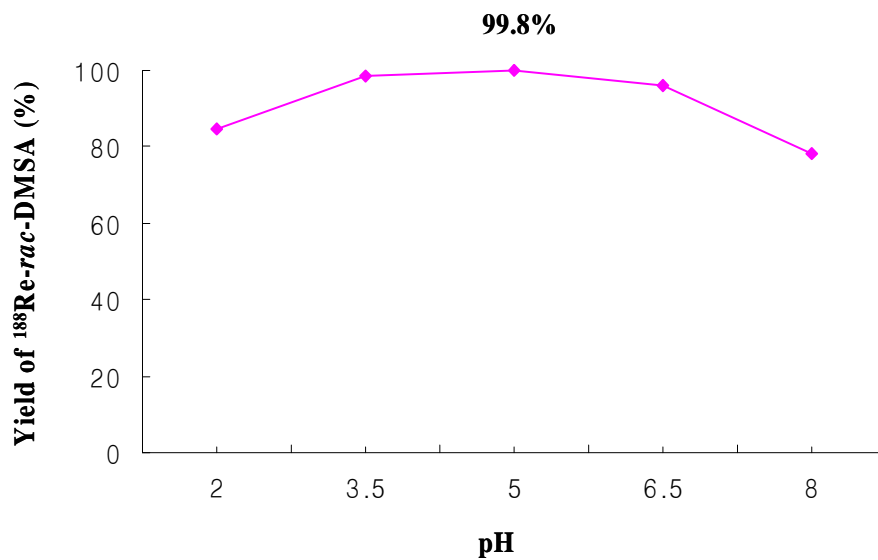


Figure 10. Effect of pH on the yield of $^{188}\text{Re(V)-rac-DMSA}$.

($^{188}\text{ReO}_4^-$: 4 mCi, DMSA : 15 mg/ml, MBS : 60 mg/ml, 80°C, 1h)

3. Chromatographic analysis of $^{188}\text{Re(V)}$ -DMSA complexes

The radiolabeling yield and purity of $^{188}\text{Re(V)}$ -DMSA complexes were determined by TLC and HPLC.

In the conditions described for chromatographic system, $^{188}\text{ReO}_4^-$ and hydrolyzed-reduced ^{188}Re (^{188}Re -colloid) are separated from the labelling mixture and their R_f values are coincided with those of references.[22,23] When normal saline is used as mobile phase, ^{188}Re -colloid remain at the origin ($R_f = 0$) while $^{188}\text{Re(V)}$ -DMSA complexes and free perrhenate migrate with the solvent front ($R_f = 1$). TLC in acetone, $^{188}\text{Re(V)}$ -DMSA complexes and ^{188}Re -colloid remain at the origin ($R_f = 0$), whereas only free perrhenate moves to solvent front ($R_f = 1$). The results of TLC are represented as normalized chromatogram (Fig. 11, 12).

The HPLC analysis of $^{188}\text{Re(V)}$ -*meso*-DMSA and $^{188}\text{Re(V)}$ -*rac*-DMSA was performed with the optimal labeling conditions (Table 1). The chromatogram of $^{188}\text{Re(V)}$ -*meso*-DMSA was shown the isomeric composition (Fig. 13). *Anti*-, *syn-endo*- and *syn-exo*-isomers eluted with retention times of 9.5 ± 0.2 , 13.5 ± 0.5 , and 16.5 ± 0.3 min, respectively. The unknown small peak between the *anti*- and *syn-endo*-isomers was also present as reported earlier.[22,23] The HPLC pattern of $^{188}\text{Re(V)}$ -*rac*-DMSA was shown single peak with a retention times of 1.9 ± 0.2 min (Fig. 14).

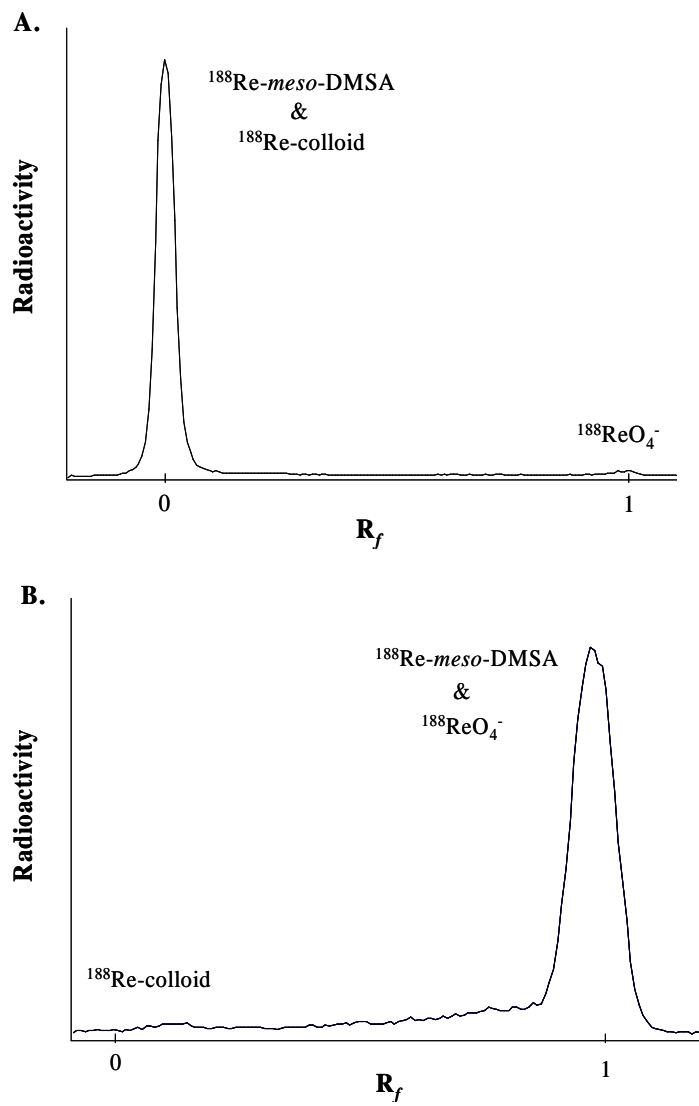


Figure 11. Radiochromatogram of $^{188}\text{Re(V)-meso-DMSA}$.

(TLC conditions of mobile phase : (A) acetone, (B) normal saline)

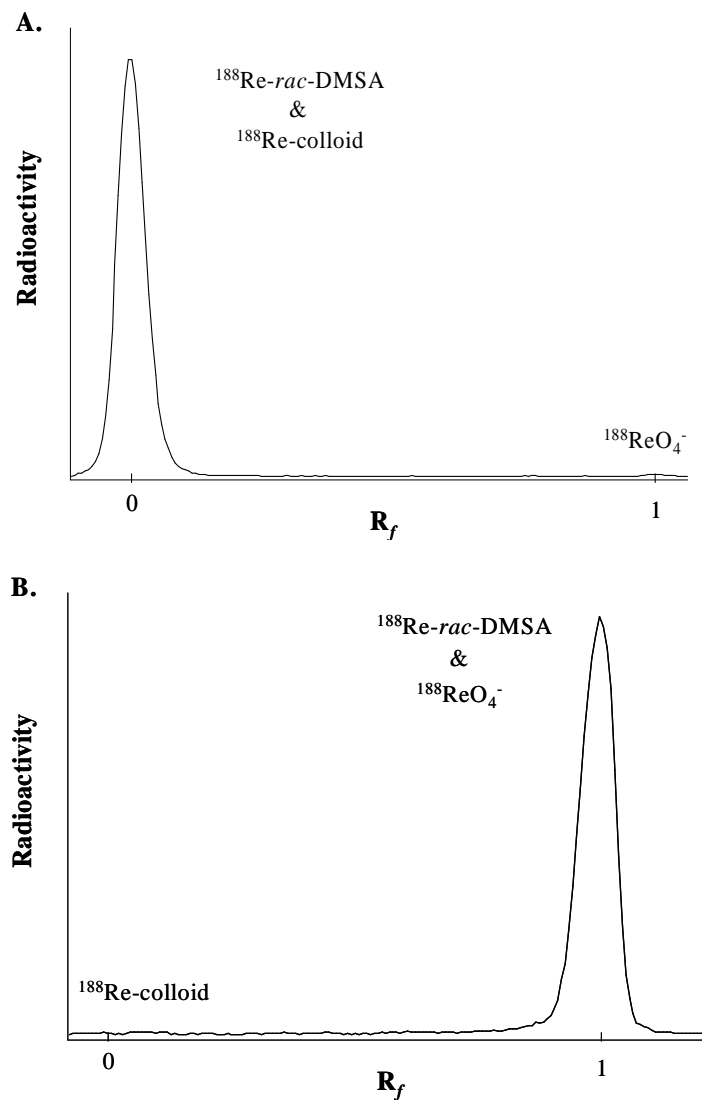


Figure 12. Radiochromatogram of $^{188}\text{Re(V)-rac-DMSA}$.

(TLC conditions of mobile phase : (A) acetone, (B) normal saline)

Table 1. The optimal conditions for the preparation of $^{188}\text{Re(V)}$ -DMSA complexes

Optimization of	$^{188}\text{Re-}meso\text{-DMSA}$	$^{188}\text{Re-}rac\text{-DMSA}$
DMSA (mg/ml)	10	15
metabicyclite (mg/ml)	30	60
pH	3.5	5.0
$^{188}\text{ReO}_4^-$	4 mCi	4 mCi
reaction temp.	80°C	80°C
reaction time	60 min.	60 min.

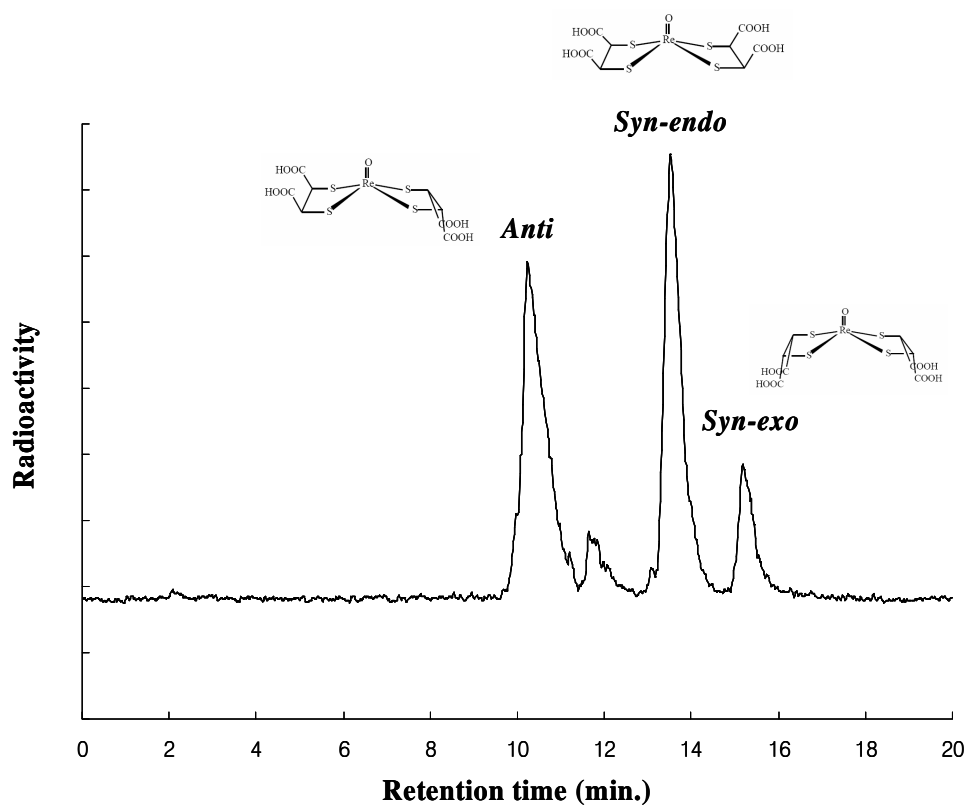


Figure 13. HPLC chromatogram of $^{188}\text{Re(V)}$ -*meso*-DMSA.

(Mobile phase : water with 0.1% trifluoroacetic acid (solvent A), acetonitrile with 0.1% trifluoroacetic acid (solvent B), Stationary phase : Hamilton PRP-1 column, Flow rate : 1 mL/min, Absorbance detection : 340 nm)

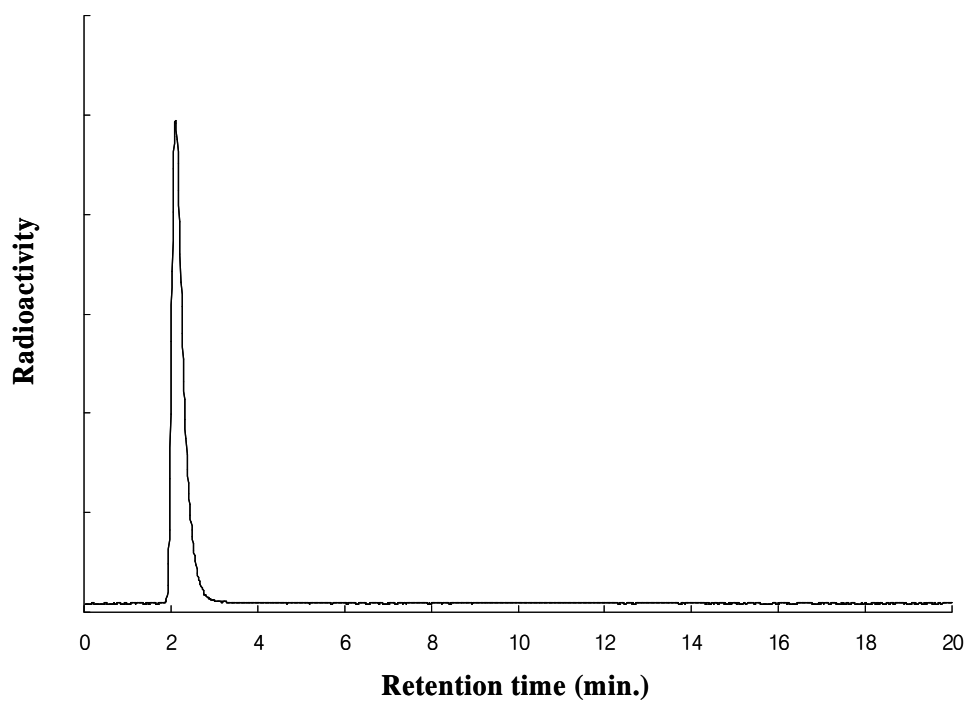


Figure 14. HPLC chromatogram of $^{188}\text{Re(V)-rac-DMSA}$.

(Mobile phase : water with 0.1% trifluoroacetic acid (solvent A), acetonitrile with 0.1% trifluoroacetic acid (solvent B), Stationary phase : Hamilton PRP-1 column, Flow rate : 1 mL/min, Absorbance detection : 340 nm)

4. Biochemical Characterizations of $^{188}\text{Re(V)}$ -DMSA complexes

The optimal radiolabeling conditions were used in product preparation for *in vitro* stability, lipophilicity and protein bindability.

The *in vitro* stability of the ^{188}Re -DMSA complexes was studied at various time points. After adjusting the pH to 7.4, the complexes were incubated for 48 h at room temperature and analyzed by TLC. Both $^{188}\text{Re(V)}$ -*meso*-DMSA and $^{188}\text{Re(V)}$ -*rac*-DMSA were found to retain the radiochemical purity as high as 99% even after 24 h (Fig. 15).

The lipophilicity was characterized by the partition coefficient (P). P is defined as the equilibrium concentration ratio of a solute between the organic and aqueous phase. The results indicated that $^{188}\text{Re(V)}$ -*meso*-DMSA was more lipophilic than *rac* complexes (Table 2).

The protein bindabilities of $^{188}\text{Re(V)}$ -DMSA complexes were summarized in Table 2. The results showed that the protein bindability of $^{188}\text{Re(V)}$ -*meso*-DMSA was 67.7%. $^{188}\text{Re(V)}$ -*rac*-DMSA was evaluated similar bound percent values compared with $^{188}\text{Re(V)}$ -*meso*-DMSA.

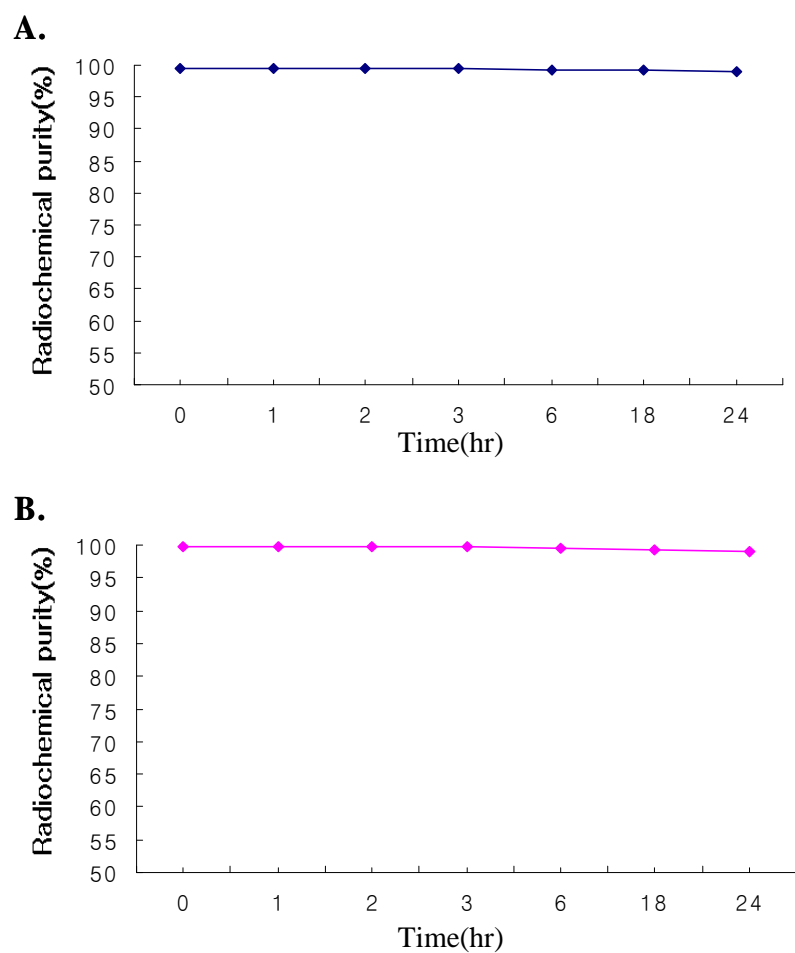


Figure 15. *in vitro* Stability test of $^{188}\text{Re(V)}$ -DMSA complexes.

(A: $^{188}\text{Re(V)}$ -*meso*-DMSA, B : $^{188}\text{Re(V)}$ -*rac*-DMSA)

Table 2. Distribution between organic and aqueous phase and protein bindability of $^{188}\text{Re(V)}$ -DMSA complexes

	$^{188}\text{Re-}meso\text{-DMSA}$	$^{188}\text{Re-}rac\text{-DMSA}$
Distribution*	0.027	0.005
Protein bindability	67.7%	66.4%

* Distribution was obtained by logarithm of the partition coefficients of $^{188}\text{Re(V)}$ -DMSA complexes.

5. Organ Distribution of $^{188}\text{Re(V)}$ -DMSA complexes in nude mouse bearing PC-12

$^{188}\text{Re(V)}$ -*meso*-DMSA and $^{188}\text{Re(V)}$ -*rac*-DMSA were intravenously injected in PC-12 neuroendocrine tumor bearing mice and the average uptake in blood, liver, lung, spleen, kidney, stomach, intestine, thyroid, muscle, bone (represented by femur), and tumor was determined.

Organ distribution of $^{188}\text{Re(V)}$ -*meso*-DMSA and $^{188}\text{Re(V)}$ -*rac*-DMSA are presented in Table 3 (Fig.16) and Table 4 (Fig.17). The results showed that approximately 90% radioactivity of $^{188}\text{Re(V)}$ -*meso*-DMSA and $^{188}\text{Re(V)}$ -*rac*-DMSA was excreted via the urinary tract within 1 h post-injection. $^{188}\text{Re(V)}$ -*meso*-DMSA showed faster blood clearance than $^{188}\text{Re(V)}$ -*rac*-DMSA at early time points, however, the radioactivity values in blood of two complexes were almost similar at 24 h post-injection. $^{188}\text{Re(V)}$ -*meso*-DMSA was localized in bone with high affinity and % dose per gram of tissue at stomach was 7.23, 3.78 and 1.88 at 1 h, 3 h and 24 h, respectively. $^{188}\text{Re(V)}$ -*rac*-DMSA was accumulated in kidney and stomach with relatively high affinity. Percent dose per gram of tissue at stomach for $^{188}\text{Re(V)}$ -*rac*-DMSA was 3.98, 1.78 and 0.24 at 1 h, 3 h and 24 h, respectively. At the values at 1 h for kidney was 2.94, but it decreased to 0.51 after 24 h. Table 4 showed that % dose per gram of tissue at tumor was higher than the values at other organs except kidney, stomach and bone at 1 h.

Table 3. Biodistribution of ^{188}Re -*meso*-DMSA in nude mouse bearing PC-12

Organ	Unit : %ID/g *		
	1h	3h	24h
Blood	0.32±0.04	0.07±0.01	0.01±0.00
Liver	0.41±0.03	0.26±0.05	0.23±0.02
Lung	0.36±0.04	0.10±0.01	0.05±0.02
Spleen	0.18±0.04	0.12±0.07	0.06±0.01
Kidney	1.16±0.22	0.75±0.13	0.45±0.12
Stomach	0.20±0.03	0.25±0.09	0.06±0.01
S. Intestine	0.17±0.03	0.42±0.27	0.04±0.00
L. Intestine	0.09±0.01	0.90±0.25	0.19±0.09
Thyroid	0.04±0.00	0.02±0.00	0.01±0.00
Muscle	0.32±0.15	0.19±0.13	0.05±0.03
Femur	7.23±1.61	3.78±0.63	1.88±0.28
Tumor	0.40±0.12	0.16±0.06	0.09±0.01

* Values at each time point represent the mean \pm s.d. of percentage of injected dose per gram of tissue weight (n=3 or 4).

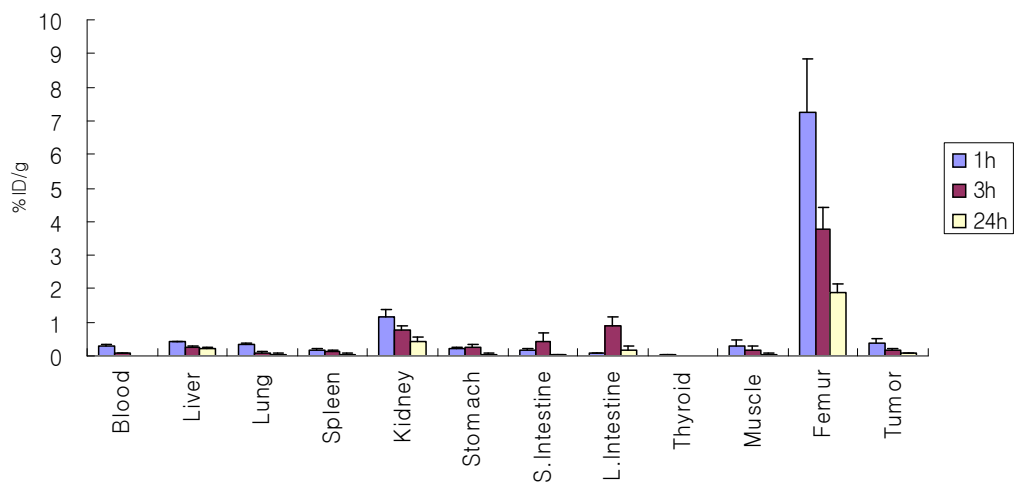


Figure 16. Biodistribution of $^{188}\text{Re}(\text{V})\text{-meso-DMSA}$ in nude mouse bearing PC-12.

Table 4. Biodistribution of $^{188}\text{Re-rac-DMSA}$ in nude mouse bearing PC-12

Organ	Unit : %ID/g *		
	1h	3h	24h
Blood	0.85±0.24	0.19±0.03	0.02±0.01
Liver	0.92±0.31	0.41±0.05	0.14±0.01
Lung	0.93±0.28	0.22±0.03	0.06±0.00
Spleen	0.36±0.10	0.13±0.02	0.06±0.01
Kidney	2.94±0.91	0.99±0.08	0.51±0.04
Stomach	3.98±0.22	1.78±0.30	0.24±0.11
S. Intestine	0.54±0.13	0.17±0.05	0.04±0.01
L. Intestine	0.32±0.22	0.15±0.04	0.22±0.02
Thyroid	0.17±0.04	0.07±0.02	0.01±0.00
Muscle	0.60±0.16	0.18±0.09	0.03±0.00
Femur	1.95±0.85	1.00±0.12	0.28±0.02
Tumor	1.15±0.53	0.33±0.08	0.10±0.02

* Values at each time point represent the mean \pm s.d. of percentage of injected dose per gram of tissue weight (n=3 or 4).

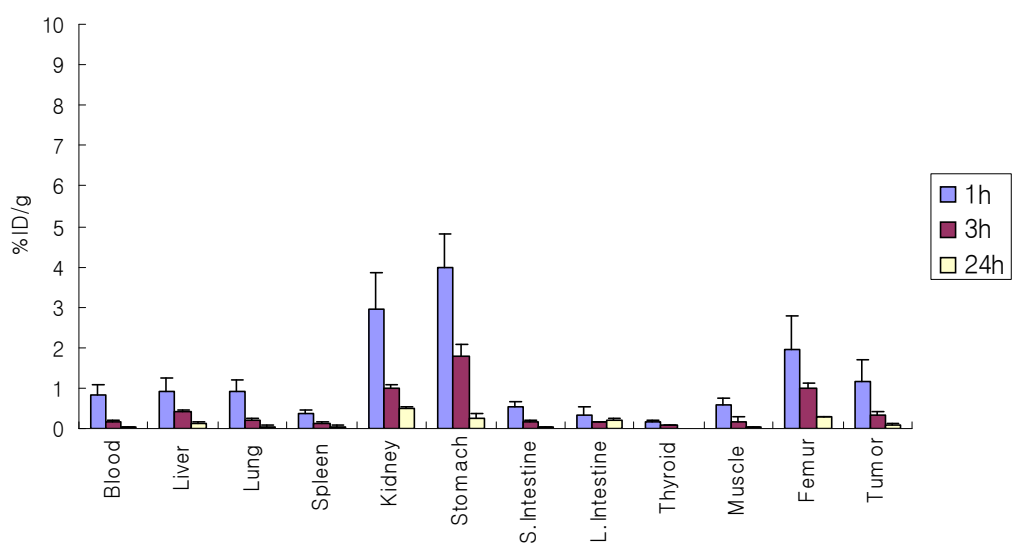


Figure 17. Biodistribution of $^{188}\text{Re}(\text{V})\text{-rac-DMSA}$ in nude mouse bearing PC-12.

Organ per tissue ratios of $^{188}\text{Re}(\text{V})\text{-meso-DMSA}$ and $^{188}\text{Re}(\text{V})\text{-rac-DMSA}$ are presented in Table 5. The tumor-to-blood ratio of $^{188}\text{Re}(\text{V})\text{-meso-DMSA}$ reached 1.30 ± 0.48 at 1h post-injection, which then increased 6.69 ± 0.82 at 24 h. $^{188}\text{Re}(\text{V})\text{-rac-DMSA}$ also increased from 1.31 ± 0.31 to 5.98 ± 0.69 at the same time point. The tumor-to-muscle ratio of $^{188}\text{Re}(\text{V})\text{-meso-DMSA}$ was 2.02 ± 1.07 at 24 h, whereas that of $^{188}\text{Re}(\text{V})\text{-rac-DMSA}$ reached 3.41 ± 0.64 at this time point.

6. Gamma camera image of $^{188}\text{Re}(\text{V})\text{-DMSA}$ complexes in nude mouse bearing PC-12

PC-12 neuroendocrine tumored nude mice were imaged using gamma camera at 1, 3 and 6 h, respectively after intravenous injection of $^{188}\text{Re}(\text{V})\text{-DMSA}$ complexes (Fig. 18 and Fig. 19).

Consistent with biodistribution data, the radioactivity of $^{188}\text{Re}(\text{V})\text{-meso-DMSA}$ was highly accumulated in bone and the radioactivity of $^{188}\text{Re}(\text{V})\text{-rac-DMSA}$ was clearly visible in kidney, stomach and tumor region.

Table 5. Organ per Tissue ratios of $^{188}\text{Re(V)}$ -DMSA complexes

Organ/Tissue	1h	3h	24h
$^{188}\text{Re-meso-DMSA}$			
Tumor/Blood ratio	1.30±0.31	2.15±0.84	6.69±0.82
Tumor/Muscle ratio	1.45 ±0.77	1.25±1.16	2.02±1.08
$^{188}\text{Re-rac-DMSA}$			
Tumor/Blood ratio	1.31±0.31	1.80±0.56	5.98±0.69
Tumor/Muscle ratio	1.84 ±0.52	2.01±0.77	3.41±0.64

* Mean (\pm S.D.) for 4 animals in each measurement.

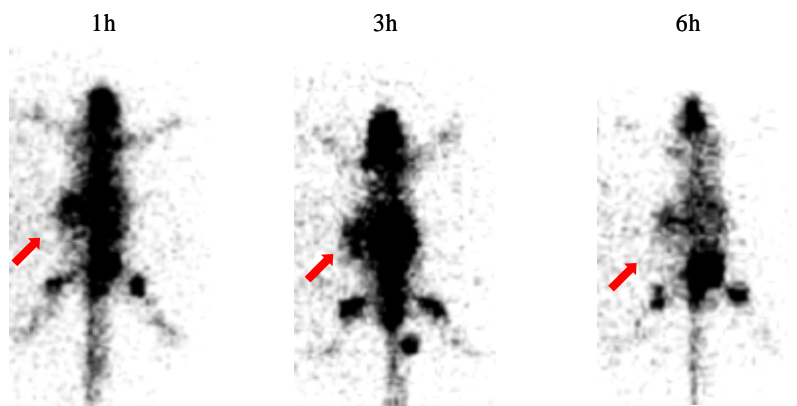


Figure 18. Gamma camera image of $^{188}\text{Re}(\text{V})\text{-meso-DMSA}$ in nude mouse bearing PC-12. (The arrows indicate the tumor region)

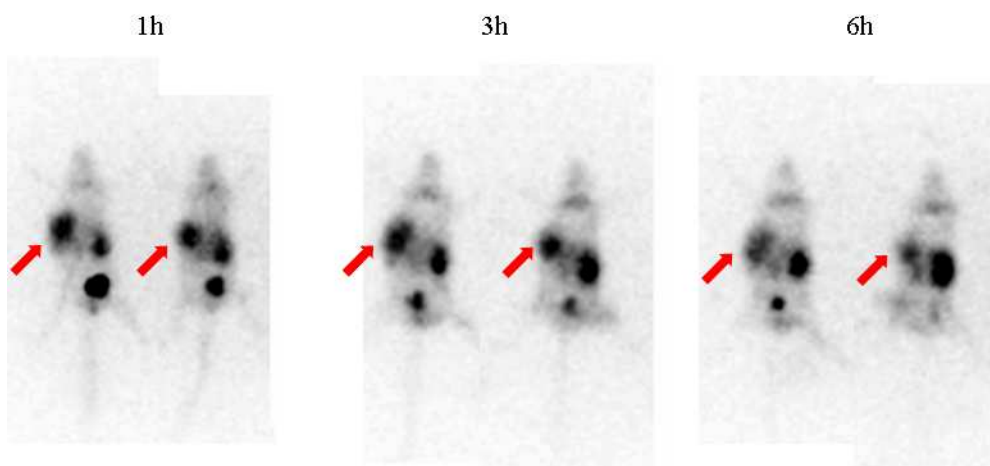


Figure 19. Gamma camera image of $^{188}\text{Re}(\text{V})\text{-rac-DMSA}$ in nude mouse bearing PC-12. (The arrows indicate the tumor region)

IV. DISCUSSION

$^{99m}\text{Tc(V)}$ -DMSA been widely used in the diagnosis of head and neck tumors, soft tissue tumors, osteosarcoma and bone metastases.[24-28] Because of its structural equivalence with the technetium analog, $^{188}\text{Re(V)}$ -DMSA has been found to have almost same biological behavior and localize in same target tissues.[3,19] Especially, since $^{99m}\text{Tc(V)}$ -DMSA is selectively accumulated in MTC as reported earlier[16-18], $^{188}\text{Re(V)}$ -DMSA might have the possibility to be used for NETs diagnosis and therapy.

DMSA exists in *meso* and *rac* form. Since *rac*-2,3-DMSA was not commercially available, it was synthesized and two isomeric $^{188}\text{Re(V)}$ -DMSA complexes were prepared separately. Several experiments were carried out to optimize the labeling conditions for obtaining a maximum yield of $^{188}\text{Re(V)}$ -DMSA complexes. Both $^{188}\text{Re(V)}$ -*meso*-DMSA and $^{188}\text{Re(V)}$ -*rac*-DMSA were prepared in high yields (>99.5%). Generally, preparation of $^{99m}\text{Tc(V)}$ -DMSA and $^{186/188}\text{Re(V)}$ -DMSA for clinical studied is performed using stannous chloride (SnCl_2) as the reducing agent.[29-32] However, the previous studies showed a significantly decreased kidney uptake in case of using the tin-free $^{188}\text{Re(V)}$ -*meso*-DMSA.[20-22] For this reason, sodium metabisulfite was used as the reducing agent instead of SnCl_2 for the preparation of $^{188}\text{Re(V)}$ -DMSA complexes.

The optimal conditions for maximum yields were significantly different (Table

1). $^{188}\text{Re(V)-rac-DMSA}$ was needed a higher concentration of MBS and DMSA than $^{188}\text{Re(V)-meso-DMSA}$. In addition, although the maximum yield of $^{188}\text{Re(V)-meso-DMSA}$ was obtained at strong acidic conditions (pH 2-3.5), $^{188}\text{Re(V)-rac-DMSA}$ showed high labeling efficiency in more weaker acidic condition (pH 5). Radiolabeling yield of $^{188}\text{Re(V)-meso-DMSA}$ was rapidly decreased when the pH value was higher than pH 5. However, labeling yield of $^{188}\text{Re(V)-rac-DMSA}$ was as high as 80% even at pH 8. The radiolabeling has been commonly performed at 100°C , however, two isomeric $^{188}\text{Re(V)-DMSA}$ complexes were prepared at 80°C in this study. Because the early studies reported that *racemic* form is isomerized to the *meso* form at high temperature.[10]

The HPLC pattern of $^{188}\text{Re(V)-meso-DMSA}$ showed three main isomers and unknown forth structure as reported earlier.[22,23] $^{188}\text{Re(V)-rac-DMSA}$ eluted as a single peak, which may be attribute to the high hydrophilic nature of *rac-2,3-DMSA*.

Biochemical properties of two isomeric $^{188}\text{Re(V)-DMSA}$ complexes such as *in vitro* stability, lipophilicity and protein bindability were investigated to characterize these complexes. Both $^{188}\text{Re(V)-meso-DMSA}$ and $^{188}\text{Re(V)-rac-DMSA}$ were showed excellent stability even at room temperature for 24 h. In lipophilicity test, *meso* complexes was more lipophilic than *rac* complexes. The protein bindability of $^{188}\text{Re(V)-meso-DMSA}$ was evaluated similar bound percent values compared with $^{188}\text{Re(V)-rac-DMSA}$. Protein binding activity of the radioactive compounds is basic factor to investigate their biological behaviors *in vivo*. If a radioactive drug is injected into the body, it is mixed

with blood and can be reacted with the proteins in the blood. The nonprotein-bound and molecular weights of less than 5,000 compounds are usually rapidly excreted by glomerular filtration via kidney. Our data obtained from protein bindability would indicate that both $^{188}\text{Re(V)-meso-DMSA}$ and $^{188}\text{Re(V)-rac-DMSA}$ are excreted at a similar speed by kidney and similar biological behaviors was also expected.

The organ distribution patterns of $^{188}\text{Re(V)-meso-DMSA}$ were similar with that of $^{188}\text{Re(V)-rac-DMSA}$ in the tumor-bearing mouse model, except in bone, stomach and tumor. The biosistribution data of $^{188}\text{Re(V)-meso-DMSA}$ showed high accumulation in bone similar to the preliminary study[32], whereas $^{188}\text{Re(V)-rac-DMSA}$ observed relatively lower bone uptake. This result suggest that $^{188}\text{Re(V)-rac-DMSA}$ can be showed less side effect than $^{188}\text{Re(V)-meso-DMSA}$ because of lower bone uptake. In case of tumor and stomach uptake, $^{188}\text{Re(V)-rac-DMSA}$ was much higher than $^{188}\text{Re(V)-meso-DMSA}$ at all time points. In addition, biodistribution data of this study also showed the much lower kidney uptake as compared to the tin-containing $^{188}\text{Re(V)-meso-DMSA}$. The tumor-to-blood ratio of two isomeric $^{188}\text{Re(V)-DMSA}$ complexes showed similar pattern.

In this study, our *in vitro* and *in vivo* data proved that $^{188}\text{Re(V)-rac-DMSA}$ has different physicochemical properties as compared with $^{188}\text{Re(V)-meso-DMSA}$. The differences may attribute to the nature of *meso*-2,3-DMSA and *rac*-2,3-DMSA. In the crystal lattice, the *rac*-2,3-DMSA exists as a double-stranded structure because of the staggered gauche configuration of individual molecules, however, the *meso*-2,3-DMSA form a single strand in

which each molecule exists in an anti configuration.[10] For this reason *rac*-2,3-DMSA has higher solubility in water, strongly acidic solutions and in organic solvents than *meso*-2,3-DMSA. These conformational difference may also affected when *meso*-2,3-DMSA and *rac*-2,3-DMSA form the complexes with ^{188}Re .

V. CONCLUSION

The two isomeric $^{188}\text{Re(V)}$ -DMSA (dimercaptosuccinic acid) complexes were prepared and compared in *in vitro* and *in vivo* models to evaluate the possibility as a diagnostic and therapeutic agent for neuroendocrine tumor therapy.

rac-2,3-DMSA was synthesized from acetylenedicarboxylic acid and thioacetic acid. The $^{188}\text{Re(V)}$ -*meso*-DMSA and $^{188}\text{Re(V)}$ -*rac*-DMSA were prepared controlling pH and the concentration of DMSA and sodium metabisulfite (MBS) to investigate the optimized conditions. MBS was used as the reducing agent to reduce the kidney uptake. $^{188}\text{Re(V)}$ -*meso*-DMSA showed high labeling efficiency at pH 2, whereas $^{188}\text{Re(V)}$ -*rac*-DMSA was prepared at pH 5. $^{188}\text{Re(V)}$ -*rac*-DMSA needed more higher concentration of DMSA and MBS than $^{188}\text{Re(V)}$ -*meso*-DMSA for maximum yields. Two isomeric $^{188}\text{Re(V)}$ -DMSA complexes showed excellent radiochemical purity and high excellent stability even at room temperature. $^{188}\text{Re(V)}$ -*meso*-DMSA was more lipophilic than *rac* complexes and the protein bindability of $^{188}\text{Re(V)}$ -*meso*-DMSA was almost similar with $^{188}\text{Re(V)}$ -*rac*-DMSA.

The biodistribution studies of two isomeric $^{188}\text{Re(V)}$ -DMSA complexes was examined in BALB/c nude mice bearing PC-12 tumor. Both $^{188}\text{Re(V)}$ -*meso*-DMSA and $^{188}\text{Re(V)}$ -*rac*-DMSA showed rapid renal clearance. $^{188}\text{Re(V)}$ -*meso*-DMSA was highly accumulated in bone, whereas $^{188}\text{Re(V)}$ -*rac*-DMSA was relatively highly accumulated in stomach and kidney compared with other organ. Tumor uptake of $^{188}\text{Re(V)}$ -*rac*-DMSA was much higher than

$^{188}\text{Re}(\text{V})$ -*meso*-DMSA at 1 h and 3 h. The gamma camera image of $^{188}\text{Re}(\text{V})$ -*rac*-DMSA showed more selectively localized than *meso* complexes in tumor region. These results suggest that $^{188}\text{Re}(\text{V})$ -*rac*-DMSA may be more effective and have better potential than $^{188}\text{Re}(\text{V})$ -*meso*-DMSA as a diagnostic and therapeutic agent for treatment of neuroendocrine tumor.

VI. REFERENCE

1. Knapp, F.F., JR. Use of Rhenium-188 for Cancer Treatment. *Cancer Biotherapy and Radiopharm* 1998; 13: 337-349.
2. Knapp, F.F., JR., Beets, A.L., Guhlke, S., Zamora, P.O., Bender, H., Palmedo, H., Biersack, H.-J. Development of the Alumina-Based Tungsten-188/Rhenium-188 Generator and Use of Rhenium-188-Labeled Radiopharmaceuticals for Cancer Treatment. *Anticancer Res.* 1997; 17: 1783-1796.
3. Bolzati C, Boschi A, Ucelli L, Duatti A, Franceschini R, Piffanelli A. An alternative approach to the preparation of ^{188}Re radiopharmaceuticals from generator-produced [$^{188}\text{ReO}_4$]: efficient synthesis of $^{188}\text{Re(V)}$ -meso-2,3-dimercaptosuccinic acid. *Nucl Med Biol* 2000; 27: 309-314.
4. Gerecke M., Friedheim, E.A.H., Brossi, A. Studies of 2,3-Dimercaptosuccinic Acid. *Helv. Chim. Acta* 1961; 44: 955-960.
5. Agren A., Schwarzenbach G. Die Komplexbildung des Zinks mit Dithioweinsäure. *Helv. Chim. Acta* 1955; 38: 1920-1930.
6. Kostial K., Restek-Samaržija, Blanuša M., Piasek M., Prester Lj. Racemic-2,3-dimercaptosuccinic Acid for Inorganic Mercury Mobilization in Rats. *J. Appl. Toxicol.* 1996; 17: 71-74.

7. Aposhian H.V. DMSA and DMPS-Water soluble Antidotes for Heavy Metal Poisoning *Annu. Rev. Pharmacol. Toxicol.* 1983; 23: 193-215.
8. Aposhian H.V. *meso*-2,3-Dimercaptosuccinic Acid : chemical, Pharmacological and Toxicological Properties of an Orally Effective Metal Chelating Agent. *Annu. Rev. Pharmacol. Toxicol.* 1990; 30: 279-306.
9. Fang, X., Fernando, Q. Stereoisomeric selectivity of 2,3-dimercaptosuccinic acids in chelation therapy for lead poisoning. *Chem. Res. Toxicol* 1995; 8: 525-536.
10. Fang X, Fernando Q. Synthesis, structure and properties of *rac*-2,3-dimercaptosuccinic acid, a potentially useful chelating agent for toxic metals. *Chem Res Toxicol* 1994; 7: 148-156.
11. Rindi G, Villanacci V, Ubiali A, Scarpa A. Endocrine tumors of the digestive tract and pancreas: histogenesis, diagnosis and molecular basis. *Expert Rev Mol Diagn* 2001; 1: 323-333.
12. Kaltsas GA, Besser GM, Grossman AB. The diagnosis and medical management of advanced neuroendocrine tumors. *Endocr Rev* 2004; 25: 458-511.
13. Solcia E, Kloppel G, Sobin LH. Histological typing of endocrine tumours. 2nd ed. Heidelberg: World Health Organization, 2000

14. Vittoria Rufini, Maria Lucia Calcagni, Richard P. Baum. Imaging of Neuroendocrine Tumors. *Semin Nucl Med* 2006; 36: 228-247.
15. Brahm Shapiro, Milton D. Gross, Barry Shulkin. Radioisotope diagnosis and therapy of malignant pheochromocytoma. *Trends Endocrinol Metabol* 2001; 12: 469-475.
16. Ohta H, Yamamoto K, Endo K, et al. A new imaging agent for medullary carcinoma of the thyroid. *J Nucl Med* 1984; 25: 323-325.
17. Patel MC, Patel RB, Ramanathan P, Ramamoorthy N, Krishna BA, Sharma SM. Clinical evaluation of $^{99m}\text{Tc}(\text{V})$ -dimercaptosuccinic acid (DMSA) for imaging medullary carcinoma of the thyroid and its metastases. *Eur J Nucl Med* 1988; 13: 507-510.
18. Clarke S.E.M., Lazarus CR, Wraight P, Sampson C, Maisey MN. Pentavalent [^{99m}Tc]DMSA, [^{131}I]MIBG, and [^{99m}Tc]MDP an evaluation of three imaging techniques in patients with medullary carcinoma of the thyroid. *J Nucl Med* 1988; 29: 33-38.
19. Bisunadan M. M., Blower P. J., Clarke S. E. M., Singh J. and Went M. J. Synthesis and characterization of [^{186}Re]rhenium(V)dimercaptosuccinic acid : A possible tumour radiotherapy agent. *Appl. Radiat. Isotopes* 1991; 42: 167-171.

20. Blower PJ, Singh J, Clarke SEM, Bisunadan MM, Went MJ. Pentavalent ^{186}Re -DMSA: a possible tumour therapy agent. *J Nucl Med* 1990; 31: 768.
21. Gerecke, M., Friedheim, E. A.H., Brossi, A. Studies of 2,3-Dimercaptosuccinic Acid. *Helv. Chim. Acta* 1961; 44: 955-996.
22. Dadachova E, Chapman J. $^{188}\text{Re(V)}$ -DMSA revisited: Preparation and biodistribution of a potential radiotherapeutic agent with low kidney uptake. *J Nucl Med Commun* 1998; 19: 173-181.
23. Kothari K, Satpati D, Mukherjee A. Kidney uptake of $^{186/188}\text{Re(V)}$ -DMSA is significantly reduced when the reducing agent is changed from stannous ion to metabisulfite *J Label Compd Radiopharm* 2002; 45: 675-686.
24. Ohta H, Endo K, Fujita T, et al. Clinical evaluation of tumour imaging using $^{99\text{m}}\text{Tc(V)}$ dimercaptosuccinic acid, a new tumour-seeking agent. *Nucl Med Commun* 1988; 9: 105-116.
25. Watkinson JC, Shaheen OH, Clarke SE. An evaluation of the uptake of technetium $^{99\text{m}}\text{Tc(V)}$ -dimercaptosuccinic acid in patients with squamous carcinoma of the head and neck. *Clin Otolaryngol* 1987; 12: 405-441.
26. Kobayashi H, Sakahara H, Hosono M, et al. Soft-tissue tumours: diagnosis with $^{99\text{m}}\text{Tc(V)}$ dimercaptosuccinic acid scintigraphy. *Radiology* 1994; 190: 277-280.
27. Ohta H, Tsuji T, Endo k, et al. SPECT images using $^{99\text{m}}\text{Tc(V)}$ -DMSA in lung metastases of osteosarcoma. *Ann Nucl Med* 1989; 3: 37-40.

28. Lam ASK, Kettle AG, O'Doherty MJ, Coakley AJC, Barrington SF, Blower PJ. Pentavalent technetium-99m-DMSA imaging in patients with bone metastases. *Nucl Med Commun* 1997; 18: 907-914.
29. Ramamoorthy N., Shetye SV, Pandey PM, Mani RS, Patel MC, Patel RB *et al.* Preparation and evaluation of $^{99m}\text{Tc(V)}$ -DMSA complex : studies in medullary carcinoma of thyroid. *Eur. J. Nucl. Med.* 1987; 12: 623
30. Allen SJ, Blake GM, McKeeney DB *et al.* $^{186}\text{Re-V}$ -DMSA : Dosimetry of a new radiopharmaceutical for therapy of medullary carcinoma of the thyroid (abstract). *Nucl Med Commun* 1990; 11: 220.
31. Xiao-Hai Jin. Development of the radiopharmaceuticals for interventional tumor therapy in china. *J Radioanal Nucl Chem Articles* 1996; 206: 17-27
32. Philip JB, Albert SKL, Michael JO, Andrew GK, Anthony JC, Knapp F.F. Pentavalent rhenium-188 dimercaptosuccinic acid for targeted radiotherapy : synthesis and preliminary animal and human studies. *Eur. J. Nucl. Med.* 1998; 25: 613-621

ABSTRACT IN KOREAN

신경 내분비 종양세포 이식 마우스에서 $^{188}\text{Re(V)-meso-DMSA}$ 와 $^{188}\text{Re(V)-rac-DMSA}$ 의 핵의학 영상

Park, Jun-Young

Dept. of Biomedical Laboratory Science

The Graduate School

Yonsei University

레늄-188 (^{188}Re , $t_{1/2} = 16.9\text{h}$)은 베타입자 ($E_{\beta} = 2.11 \text{ MeV}$)와 감마선 ($E_{\gamma} = 155 \text{ keV}$)을 방출하는 방사성동위원소로서 핵의학분야에서 진단 및 치료용으로 아주 다양하게 연구되어지고 있다. 부분입체이성질체로 존재하는 DMSA (dimercaptosuccinic acid)는 두 가지 형태인 *meso*형과 *racemic (rac)*형으로 존재한다. 본 논문에서는 *meso*형과 *rac*형의 DMSA에 방사성동위원소인 레늄-188을 표지하여 얻은 방사성표지화합들의 성질을 *in vitro*와 *in vivo*에서 비교하였으며, 그 결과를 통해 이들이 핵의학적 진단 및 치료제로서 이용 가능성이 있는지에 대해 평가하였다.

*rac-2,3-DMSA*는 acetylenedicarboxylic acid와 thioacetic acid를 시작물질로 하여 두 단계에 걸쳐 14%의 수율로 합성하였다. DMSA에 레늄-188을 표

지하기 위해 환원제로써 SnCl₂를 많이 사용하는데, 이 대신 sodium metabisulfite (MBS, Na₂S₂O₅)를 사용할 경우 신장에 대한 친화성을 줄일 수 있다는 보고가 있어 MBS를 환원제로 사용하여 표지하였다. 표지반응 결과 두 물질의 최적조건은 서로 다른 경향을 보여 주었다. ¹⁸⁸Re(V)-*meso*-DMSA는 pH 2에서 높은 표지수율을 보인 반면, ¹⁸⁸Re(V)-*rac*-DMSA는 pH 5에서 가장 높은 표지수율을 얻을 수 있었다. 그리고 높은 표지수율을 얻기 위해서는 ¹⁸⁸Re(V)-*rac*-DMSA가 좀 더 많은 양의 DMSA와 환원제를 필요로 하였다. 생화학 특성을 조사하기 위해 *in vitro*에서 이들 표지화합물들의 안정성, 친유성, 단백질 결합능들을 실험하였다. 이들 부분입체이성질성 DMSA의 ¹⁸⁸Re 착체들은 실온에서 24시간까지 안정적으로 존재하였으며, 단백질 결합능은 비슷하였으나 ¹⁸⁸Re(V)-*meso*-DMSA가 ¹⁸⁸Re(V)-*rac*-DMSA보다 더 큰 친유성을 보였다. PC-12 신경 내분비 종양 세포가 이식된 BALB/c nude mice에서 두 방사성표지화합물들의 생체분포 및 영상을 얻어 비교하였다. ¹⁸⁸Re(V)-*meso*-DMSA는 다른 장기에 비해 뼈와 신장에 많이 집적되었으나, ¹⁸⁸Re(V)-*rac*-DMSA는 위와 신장에 많이 집적되었다. 또한 ¹⁸⁸Re(V)-*rac*-DMSA가 ¹⁸⁸Re(V)-*meso*-DMSA에 비해 종양 세포에 더 많이 집적된 결과를 보여 주었다. 두 물질의 영상 비교에서는 생체분포의 결과와 일치하였는데, ¹⁸⁸Re(V)-*meso*-DMSA는 뼈, 신장, 이식된 종양 세포부위 등에 많이 집적된 영상을 확인할 수 있었고, ¹⁸⁸Re(V)-*rac*-DMSA는 위, 신장, 이식된 종양 세포부위에 집적된 뚜렷한 영상을 확인할 수 있었다.

위와 같은 결과를 통해 두 가지 부분입체이성질성 DMSA의 ¹⁸⁸Re 착체들을 신경 내분비 종양의 진단 및 치료에 적용할 경우, ¹⁸⁸Re(V)-*rac*-DMSA가 ¹⁸⁸Re(V)-*meso*-DMSA 보다 우수할 것임을 확인하였다.